Received: 29 May 2023 | Revised: 12 November 2023 | Accepted: 16 November 2023

DOI: 10.1002/hbm.26551

RESEARCH ARTICLE

WILEY

The role of the primary sensorimotor system in generalized epilepsy: Evidence from the cerebello–cerebral functional integration

Junxia Chen[1] | Sisi Jiang[1,2] | Bao Lu[1] | Jiangyan Liao[1] | Zhihuan Yang[1] | Hechun Li[1,2] | Haonan Pei[1] | Jianfu Li[1,2] | Yasser Iturria-Medina[3] | Dezhong Yao[1,2,4] | Cheng Luo[1,2,4]

[1]The Clinical Hospital of Chengdu Brain Science Institute, MOE Key Lab for Neuroinformation, School of Life Science and Technology, University of Electronic Science and Technology of China, Chengdu, P. R. China

[2]High-Field Magnetic Resonance Brain Imaging Key Laboratory of Sichuan Province, Center for Information in Medicine, University of Electronic Science and Technology of China, Chengdu, P. R. China

[3]McConnell Brain Imaging Center, Montreal Neurological Institute, McGill University, Quebec, Canada

[4]Research Unit of NeuroInformation, Chinese Academy of Medical Sciences, Chengdu, P. R. China

Correspondence
Cheng Luo, The Clinical Hospital of Chengdu Brain Science Institute, MOE Key Lab for Neuroinformation, School of Life Science and Technology, University of Electronic Science and Technology of China, Chengdu 611731, P. R. China.
Email: chengluo@uestc.edu.cn

Funding information
Chengdu Science and Technology Bureau, Grant/Award Number: 2021-YF09-00107-SN; China Postdoctoral Science Foundation, Grant/Award Number: 2021TQ0061; National Natural Science Foundation of China, Grant/Award Numbers: 61933003, U2033217, 62201133, 81960249; CAMS Innovation Fund for Medical Sciences (CIFMS), Grant/Award Number: 2019-I2M-5-039

Abstract

The interaction between cerebellum and cerebrum participates widely in function from motor processing to high-level cognitive and affective processing. Because of the motor symptom, idiopathic generalized epilepsy (IGE) patients with generalized tonic–clonic seizure have been recognized to associate with motor abnormalities, but the functional interaction in the cerebello–cerebral circuit is still poorly understood. Resting-state functional magnetic resonance imaging data were collected for 101 IGE patients and 106 healthy controls. The voxel-based functional connectivity (FC) between cerebral cortex and the cerebellum was contacted. The functional gradient and independent components analysis were applied to evaluate cerebello–cerebral functional integration on the voxel-based FC. Cerebellar motor components were further linked to cerebellar gradient. Results revealed cerebellar motor functional modules were closely related to cerebral motor components. The altered mapping of cerebral motor components to cerebellum was observed in motor module in patients with IGE. In addition, patients also showed compression in cerebello–cerebral functional gradient between motor and cognition modules. Interestingly, the contribution of the motor components to the gradient was unbalanced between bilateral primary sensorimotor components in patients: the increase was observed in cerebellar cognitive module for the dominant hemisphere primary sensorimotor, but the decrease was found in the cerebellar cognitive module for the nondominant hemisphere primary sensorimotor. The present findings suggest that the cerebral primary

motor system affects the hierarchical architecture of cerebellum, and substantially contributes to the functional integration evidence to understand the motor functional abnormality in IGE patients.

KEYWORDS
cerebello–cerebrum integration, functional connectivity, hierarchical function, idiopathic generalized epilepsy, motor

1 | INTRODUCTION

A generalized tonic–clonic seizure (GTCS) is considered clinically the most remarkable generalized seizure type in idiopathic generalized epilepsy (IGE) (Fisher et al., 2017). It is typically characterized by generalized spike–wave discharges with 2.5–5 Hz, showing systemic muscle tonic-clonus, screaming, saliva increases and outflow, and possible tongue biting, accompanied by loss of consciousness. Previous studies have illustrated significantly increased regional functional connectivity (FC) of brain networks in IGE such as sensorimotor network (SMN) (Liu et al., 2019; Zhang, Huang, Liu, Li, et al., 2021) and basal ganglia network (Luo et al., 2012), while reduced the degree centrality of FC in supplementary motor area (SMA) was also observed (Zhang, Huang, Liu, Li, et al., 2021), implying underlying cerebral motor dysfunction to respond the motor-related symptoms. Besides, the increased FC density was observed in the anterior lobe of cerebellum in IGE (Zhu et al., 2016), suggesting that the cerebellum contributes to motor dysfunction in epilepsy. Altogether, these findings suggested that the cerebral and cerebellar movement-related regions were disrupted in IGE patients. However, up to now, few studies have explored the integration of motor function between cerebrum and cerebellum in patients with IGE.

As known, motor abnormalities are the most predominant clinical symptom in patients with IGE, resulting in hyper-functionality of the motor cortices in resting, cognitive, and interictal discharge states (Tangwiriyasakul et al., 2018; Vollmar et al., 2011). The cerebellum plays an important role in sensorimotor control. It receives inputs from the cerebral cortex, as well as the spinal cord, and integrates these inputs to regulate motor activity (Fine et al., 2002). With the development of transneuronal tracking technology, it has been revealed that the motor areas of the cerebrum are anatomically connected with a specific region of the cerebellum (Kelly & Strick, 2003). For example, the hand region of primary motor cortex (both efferent and afferent polysynaptic projections) with cerebellar lobules V and VI (sensorimotor performance of the anterior lobe) and VIIb/VIII of the posterior lobe (Kelly & Strick, 2003). The output pathway of the cerebellum is mainly through Purkinje cells, which release the inhibitory neurotransmitter GABA projecting to the deep cerebellar nucleus (Krauss & Koubeissi, 2007). Functional integration indicates information interaction and coordination between different brain regions (Knosche & Tittgemeyer, 2011). At present, the resting state FC approach has been widely investigated to explore the functional interaction between cerebral networks and cerebellum (Buckner et al., 2011), suggesting the integration of motor function in the cerebello–cerebral circuit. It is worth noting that the cerebral motor function has obvious laterality. The mapping of cerebello–cerebral structural connection has a cross in the brainstem part (middle cerebellar peduncle part). The altered lateralization of motor function in cerebellum and cerebrum can reflect the abnormal integration of motor function. Moreover, the lateralization of cerebello–cerebrum motor function would be helpful to understand the role of cerebellar regions.

This study aims to evaluate the cerebello–cerebral integration in patients with IGE. Firstly, the voxel-based FC matrix between cerebral cortex and the cerebellum was contacted based on the resting fMRI. Then, two different methods were applied to analyze cerebello–cerebral functional integration on the voxel-based FC: independent components analysis (ICA) (Yuan et al., 2016) and FC gradient (Dong et al., 2020; Guell, Schmahmann, et al., 2018). The cerebral and cerebellar interaction about motor components were segregated by using Group ICA. The FC gradient was employed to characterize the overall functional hierarchy of cerebello–cerebrum. This functional hierarchy can capture how cerebellar functional networks are assembled and other key features of their interaction with cerebral cortical networks (Huntenburg et al., 2018). Finally, both methods were combined by using a model to further explore the effect of cerebello–cerebrum motor function integration on the overall functional hierarchy of cerebellum and the change of this effect in patients with IGE.

2 | MATERIALS AND METHODS

2.1 | Participants and imaging protocol

A total of 101 IGE patients (age = 24.24 ± 7.945 years, 43 females) with GTCS were recruited from the neurology department, the Affiliated Hospital of University of Electronic Science and Technology of China (UESTC). According to the International League Against Epilepsy (ILAE) (Scheffer et al., 2017), the diagnosis of all patients was established by two neurologists. Thirty-four of the 101 patients had not received any antiepileptic drugs (AED). All subjects in this study stopped taking epilepsy medications within 24 h before scanning. In addition, 106 healthy subjects (age = 25.78 ± 7.83 years, 45 females) were recruited as the control group. Written informed consent was obtained from all subjects. All study methods and the process design were approved by the local Ethics Committee of UESTC and followed the declaration of Helsinki. Detailed information on the subjects is shown in Table 1 and Table S1.

TABLE 1 Demographic characteristics of IGE patients and healthy controls.

Characteristic	IGE	HC	*p*-Values
Number	101	106	–
Age (year)	24.24±7.945	25.78±7.83	0.160[a]
Gender (M:F)	58:43	61:45	0.986[b]
AED (with:without)	67:34	–	–
Age at onset (year)	19.47 ± 8.473	–	–
Illness duration (year)	5.03±6.745	–	–
mFD (mm)	0.011±0.05	0.088±0.04	–

Abbreviations: AED, antiepileptic drug; mFD, mean frame-wise displacement.
[a]The *p*-value was obtained by a two-sample *t*-test.
[b]The *p*-value was obtained by a χ^2 test.

MRI data were acquired using a 3.0 T MRI scanner (Discovery MR750, GE). All participants were given foam padding to reduce head motion. The fMRI images were collected using an echo-planar imaging sequence. The scanning parameters were as follows: slices = 35; TR/TE = 2000 ms/30 ms; flip angle = 90°; FOV = 240 × 240mm^2; matrix size = 64 × 64and thickness = 4 mm and 255 volumes in each run. Axial anatomical T1-weighted images were attained using a 3-dimensional fast spoiled gradient echo (T1-3D FSPGR) sequence: TR = 6.012 ms, TE = 1.968 ms, FA = 9°, matrix = 256 × 256, FOV = 256 × 256mm^2, slice thickness = 1 mm, 152 slices without a gap. During scanning, the subjects were instructed to keep their eyes closed and not to fall asleep.

2.2 | Data preprocessing

Preprocessing of the fMRI data was conducted using the NIT software package (Dong et al., 2018) (https://www.neuro.uestc.edu.cn/NIT.html). The processing steps of fMRI data are as follows: (1) The first five time points were discarded due to the inhomogeneity of the magnetic field. (2) The remaining 250 volumes were corrected for temporal differences and head movement. The participants were excluded if their head motions were more than 1 mm or 1° in any direction (none of the participants was excluded). (3) Spatial normalization was performed for the image to Montreal Neurological Institute (MNI) space and the fMRI data was resampled to 3-mm isotropic resolution. (4) To remove physiological noise, head motion and white matter (WM), and cerebrospinal fluid (CSF) signals were regressed. (5) A bandpass filter (0.01–0.08 Hz) was employed. No spatial smoothing was applied because the FC analysis was performed voxel by voxel.

2.3 | Voxel-based cerebello–cerebral connectivity map

The voxel-based FC map between cerebellum (number of voxels = *N1*) and cerebrum (number of voxels = *N2*) was analyzed (Figure 1a). First, the cerebellar and cerebral masks were extracted from MRI images. The voxels of masks were resampled to $3 \times 3 \times 3\text{cm}^3$. Second, the cerebral functional map was acquired for each cerebellar voxel based on the Pearson correlation between the given cerebellar voxel and each cerebral voxel. Finally, all correlation maps (the matrix of correlation coefficient, $N1 \times N2$) were transformed to Z-scores using Fisher r-to-z algorithm, resulting in *N1* seed-based cerebral FC maps for each subject.

2.4 | Identification of motor components in cerebellum

Independent component analysis was performed on these cerebellar voxel-based FC maps to obtain specific components related to motor-network components. All the cerebellar FC data ($n \times N1 \times N2$, number of all subjects = n) of both the cases and control participants were performed group ICA with three steps. First, principal component analysis was used to decompose the dimension of FC data of each subject along the direction of *N1*. Second, the compressed data of all subjects were concatenated and decomposed into m independent components (ICs) using the infomax algorithm. The ICASSO method was further used to repeat the measurement 20 times to maintain the stability and consistency of IC decomposition. Finally, the spatial ICs (represents the cerebral spatial pattern, $m \times N2$) and the corresponding "time process" (represents the cerebellar spatial distribution, $N1 \times m$ of each subject were reconstructed by dual regression algorithm. From the decomposed ICs, k (number of selected motor components $k \leq m$) motor components (Figure 2) were identified for further analysis according to the goodness-of-fit with our previous motor mask (Luo et al., 2016).

For each subject, to obtain the relationship between each cerebellar voxel and motor components, the contribution of each motor component to each correlation map of the cerebellar voxel was evaluated (Figure 1b). First, the cerebellar correlation maps and each IC map were transformed into a one-dimensional array vector, and a multiple linear regression model was used to quantify the relationship between IC and each voxel in the cerebellum, and the coefficient (β) measures the contribution of each spatial component to the voxel-based correlation map, reflecting the mapping of each brain spatial component to the cerebellar region. Therefore, the specific linear regression model formula was given as follows:

$$y_{1(i)} = \beta_{(1,i)} \cdot V_{IC1} + \ldots + \beta_{(j,i)} V_{ICj} + \varepsilon$$

(for each voxel in the cerebellum, $i = 1,2, \ldots, N1$; for each selected motor component, $j = 1,2, \ldots, k$) y_1 represents the cerebellar FC data ($N1 \times N2$), $V_{IC}$are k motor-related spatial component maps ($k \times N2$), $\beta_{(j,i)}$ represents the contribution value of j^{th} spatial component to the map to the cerebellar correlation map of the i^{th} voxel. The *N1* voxels in the cerebellum were performed in the regression analysis (Figure 1b).

These β values were normalized to refer to cerebellar motor components. Then, spatially smoothing was performed with a 6-mm FWHM Gaussian kernel. The *t*-test was performed to acquire differences between cases and controls for each motor sub-region in the cerebellum, at $p < .05$ (FDR corrected).

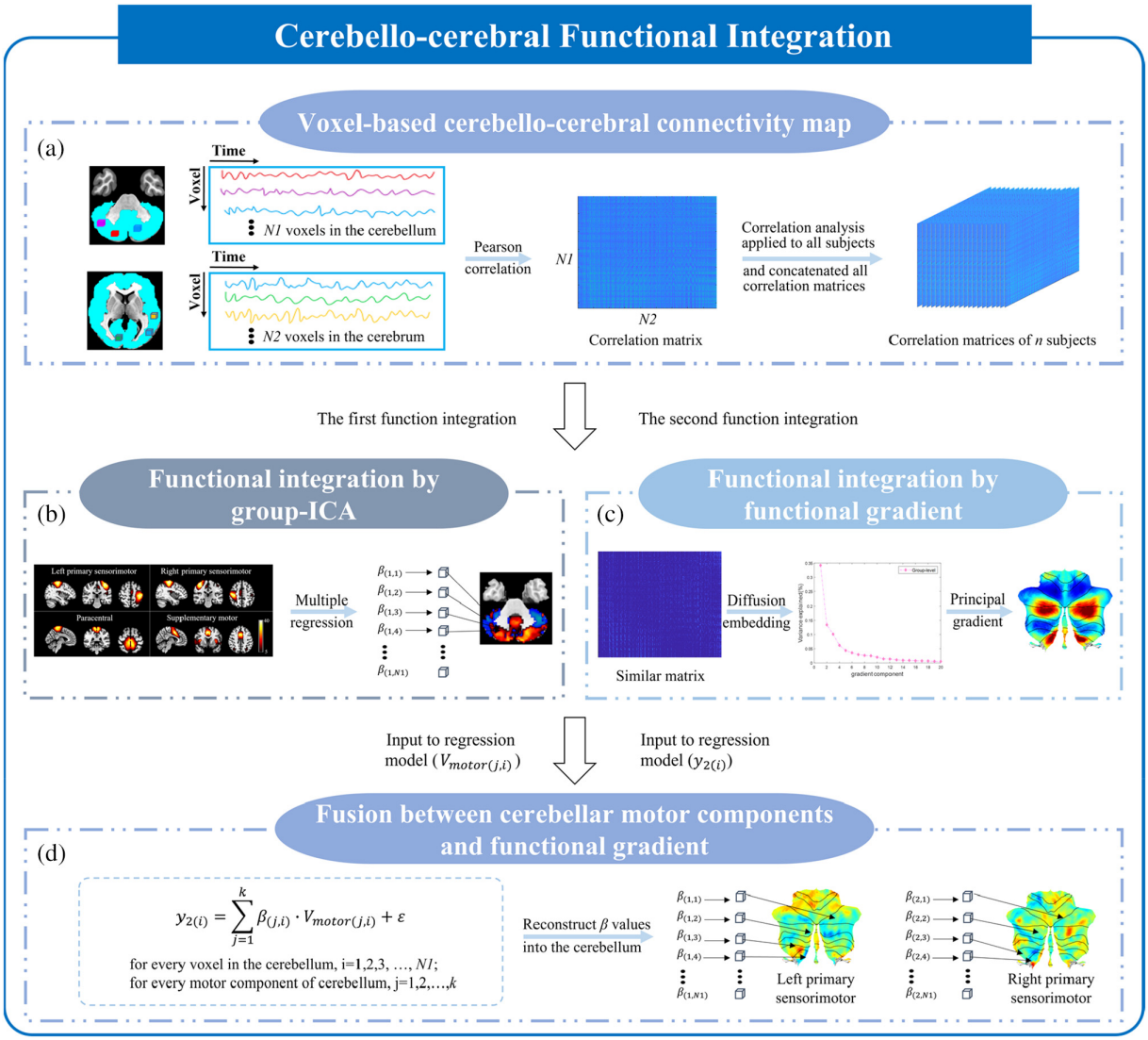

FIGURE 1 Workflow of image processing based on cerebello–cerebral functional integration. (a) Calculate the Pearson's correlation between the time series of each voxel in the cerebellum and the voxels of the cerebrum of the subject, and the correlation matrices from all subjects were concatenated. (b) Group-ICA was performed on the functional connectivity diagram to select cerebral motor components. Then the cerebral components were mapped to the cerebellum by multiple linear regression model to construct β atlas for each component. (c) The cerebello–cerebral functional connectivity matrix was transformed into a similarity matrix, and a diffusion embedding map was used to capture the explained variance that was sorted. (d) The fusion between cerebellar motor components and the functional gradient was calculated using a spatial regression model based on population covariance.

The lateralization of cerebellar motor components was also evaluated because of the lateralized feature of motor function in human cerebrum and cerebellum. First, a hemispherical symmetrical cerebellar template was built and applied to cerebellar components of all subjects. Then, the homotopic lateralized index (*LI*) voxel-wise maps were obtained. The *LI* formula was as follows:

$$LI_{(v)} = \frac{R_v - L_v}{R_v + L_v}$$

where *R* and *L* represent the right hemisphere and left hemisphere for each pair of homotopic voxels *v* ($v = 1, 2, \ldots, N3$, number of homotopic voxel pairs $= N3$). Positive lateralized index values denoted rightward lateralization. Voxel-wise *LI* map could be obtained for each cerebellar motor component of each subject. Finally, the *LI* maps were compared within each group using one-sample *t*-test.

2.5 | Cerebellar–cerebral cortical functional gradient analyses

To describe the global function of cerebellum, cerebello–cerebral functional gradient was used based on the voxel-based cerebello–cerebral FC (Figure 1c). First, based on our previous studies

(Guell, Schmahmann, et al., 2018; Margulies et al., 2016), the FC matrix ($N1 \times N2$) was thresholded, leaving only the top 10% of connections per row, whereas all others were zeroed. Second, the calculation of a cosine distance to generate a cosine similarity matrix was carried out that captures similarity connectivity profiles between each pair of voxels (between cerebellar and cerebral voxel). The diffusion mapping embedding (Coifman et al., 2005; Guo et al., 2023), a nonlinear dimensionality reduction approach was then used to identify relevant aspects of cerebral cortex and cerebellar functional organization. Diffusion mapping embedding does not define a single mosaic of a discrete network but extracts multiple continuous gradient maps, which capture the similarity of the functional connection of each voxel along a continuous space. Finally, to uncover the differences between cases and controls, a group-level gradient component template was generated by using the average connectivity matrix calculated for both groups. Procrustes rotation was performed to align components of each participant to this template. For the sake of maximizing reliability, reproducibility, and interpretability, the study focused on the first components (or principal gradient). Meanwhile, the explanatory variables of the principal gradient are shown in Figure S2. The principal gradient value was compared between cases and controls by two-sample *t*-test with an FDR-corrected $p < 0.05$ on the smoothed with a 6-mm FWHM Gaussian kernel gradient maps.

2.6 | Fusion between cerebellar motor components and functional gradient

To further explore the fusion between functional gradient and cerebellar motor components on each cerebellar voxel, the contribution of each cerebellar motor component to functional gradient was evaluated (Figure 1d). The linear regression model was used to quantify the relationship between cerebellar motor components and gradient. The formula was given as follows:

$$y_{2(i)} = \sum_{j=1}^{k} \beta_{(j,i)} \cdot V_{motor(j,i)} + \varepsilon$$

(For every voxel in the cerebellum, $i = 1,2,3, \ldots, N1$; for every motor component of cerebellum, $j = 1, \ldots, k$.) $y_{2(i)}$ represents the gradient value of the i^{th} voxel for all subjects in the group, $V_{motor(j,i)}$ represents the value of the i^{th} voxel of the j^{th} cerebellar motor component of all subjects in the group. $\beta_{(j,i)}$ represents the contribution of the i^{th} voxel of the j^{th} component of all subjects in the group to the i^{th} voxel of the gradient, and ε is the residual of the regression model. Finally, k cerebellar βmaps were attained for each group. Between-group comparisons were performed using individual permutation-based statistical testing (replacing 5000 times, $p < .005$).

Significantly, to further verify the results, the voxel-based covariance method was also applied for each subject, and the following formula was employed.

$$y_{3(s)} = \beta_{(1,s)} \cdot V_{motor(1,s)} + \ldots + \beta_{(j,s)} \cdot V_{motor(j,s)} + \varepsilon$$

(For every subject, $s = 1,2,3, \ldots, n$; for every motor component of cerebellum, $j = 1, \ldots, k$) where, $y_{3(s)}$ represents the gradient of the s^{th} subject in the group ($N1 \times 1$), $V_{motor(j,s)}$ represents the j^{th} cerebellar motor component ($N1 \times 1$) of the s^{th} subject. So, $\beta_{(j,s)}$ represents the contribution of the j^{th} cerebellar movement of the s^{th} subject to the gradient. Each subject performed the regression analysis and got k different β results. Finally, the β results obtained from the same component of all subjects in the group were connected in series for one-sample t-test, and then two-sample *t*-test was used for intergroup comparison.

2.7 | Correlations between functional interaction and clinical variables

Furthermore, the current study investigated the correlation between the altered functional interaction value (abnormal cerebellar motor components and gradient scores) and disease duration. Gender, age of onset, and whether to take AED were used as covariates to control the confounding effects.

2.8 | Validation analysis

To verify the stability of the results, a high model order ICA was performed. One hundred and fifty ICs were decomposed for cerebello–cerebral FC. Then, k cerebral motor components were selected and analyzed with the repeated analysis process.

3 | RESULTS

3.1 | Group-level ICA of voxel-based cerebello–cerebral connectivity map

According to the distribution of components in cerebral cortex, four motor components ($n = 4$) were selected from the ICA ($m = 50$ components in total), including left primary sensorimotor component (involving left precentral and postcentral gyrus), right primary sensorimotor component, SMA component, and paracentral component (Figure S1).

The cerebellar distribution corresponding to four cerebral motor components was shown in Figure 2a,b. The left primary sensorimotor component mainly corresponded to the right cerebellar motor lobules including cerebellar VI and VIIa regions. Similarly, the right primary sensorimotor component had an obvious relation with the left cerebellar motor module (VI and VIIa). The SMA component illustrated an association with the bilateral cerebellum as the primary sensorimotor area. Finally, the cerebellum sub-region related to the paracentral component encompassed a portion of the cerebellum, including the

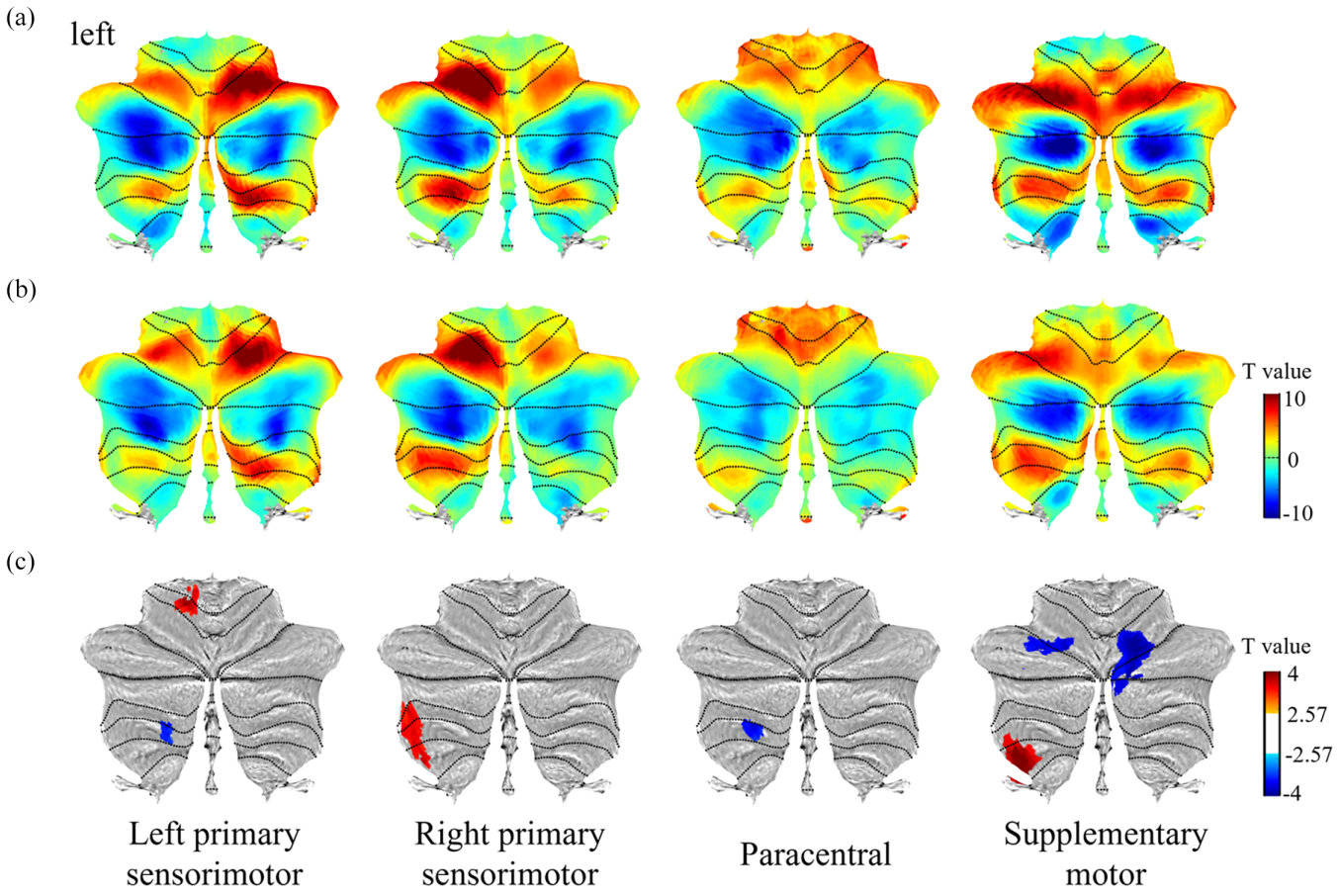

FIGURE 2 (a) In the healthy control group, different cerebral motor components corresponded to the cerebellar subregion. (b) There were different cerebrum motor components corresponding to the cerebellar subregion in patients with IGE. (c) The difference of corresponding cerebellar subregion between IGE and controls (FDR, $p < .05$).

bilateral lobules I–IV/V and small part mapping region of the lateral upper part of bilateral lobules VI. Taken together, the motor components mapping to cerebellar sub-regions were found mostly at lobules I–IV/V/VI and VIIa/VIIb. All these cerebellar regions were identified according to the spatially unbiased infratentorial template (SUIT) (Diedrichsen, 2006). Notably, there was significant lateralization in left and right primary sensorimotor components according to the results of one-sample *t*-test (Figure 3). In detail, the left primary sensorimotor was mainly right deviation in the cerebellum, while the right primary sensorimotor was located left side of the cerebellum.

A two-sample *t*-tests was employed to determine significant between-group differences ($p < .05$, FDR) in mapping of each motor component on the cerebellum (Figure 2c). Compared to HC, the IGE group showed a significantly increased connection between the left primary sensorimotor area and the left cerebellar motor lobule (V and I–IV regions). In addition, compared with HC, the mapping of the right primary sensory motor region was increased in cerebellum lobules VIIb/VIIa/VIIb in IGE. Similarly, the mapping of SMA in cerebellar lobule VIIb region was also increased (Table S2 for details).

Significantly, decreased mapping of the left primary sensorimotor area and paracentral component to left lobule VIIa was observed in

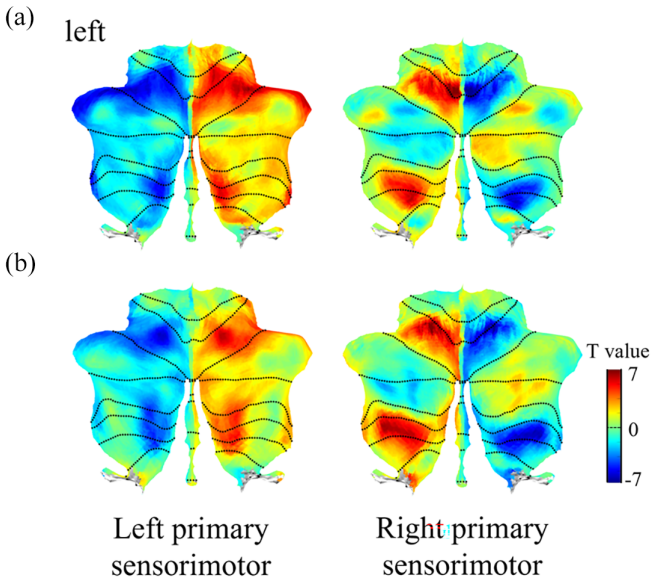

FIGURE 3 The group-level lateralized index (*LI*) resulted from voxel-wise homotopic maps of the cerebellar motor components. (a) The LI results of HC. (b) The LI results of IGE.

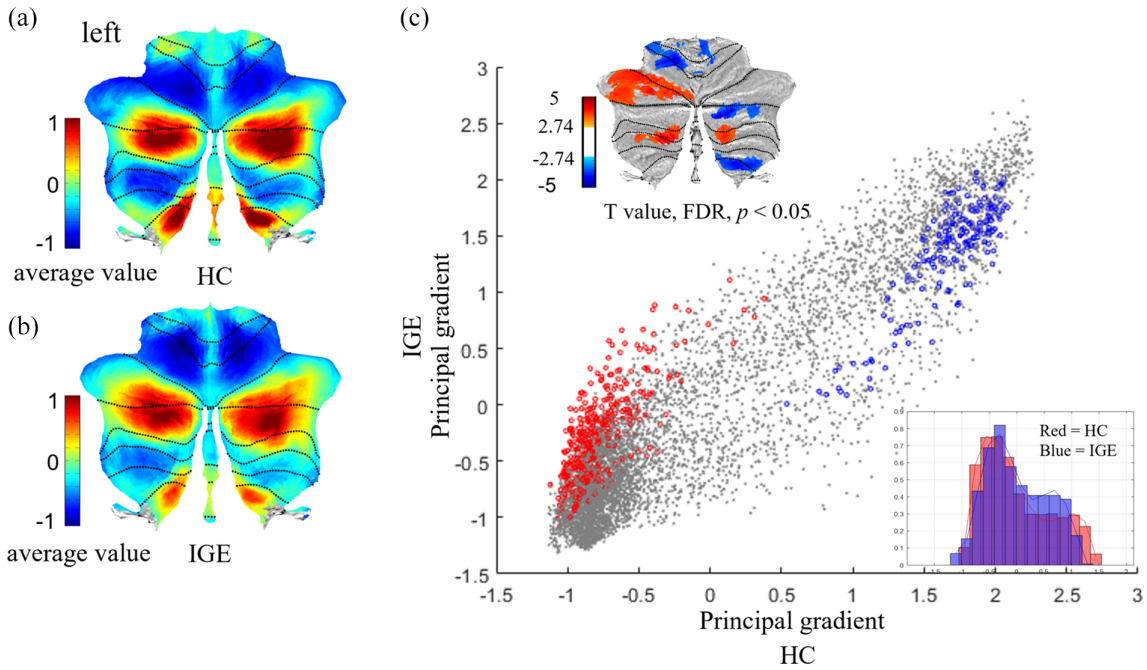

FIGURE 4 Group patterns and abnormal cerebello–cerebral principal gradient pattern in IGE. (a) Principal gradient pattern in HC. (b) Principal gradient pattern in IGE. (c) Group differences between IGE and HC. The scatter plot showed the cerebello–cerebral principal gradient of IGE (*Y*-axis) and HC (*X*-axis). The color of the scatter diagram corresponds to the group difference map was shown in the top left corner. Red represents the higher gradient value of IGE, and the blue represents the lower gradient value of IGE. The compressed gradient pattern in IGE was shown in density histograms in the bottom right corner. The result of group differences between IGE and HC was shown after FDR correction ($p < .05$).

IGE patients. The decreased corresponding association between the SMA and cerebellum was mainly located in the lobule VI and Crus I.

3.2 | Cerebello–cerebral cortex functional gradient

Within group, a similar spatial distribution of the first gradient of FC from cerebellum to cerebrum cortex in IGE and HC was shown in Figure 4, which included bilateral motor lobules (I–IV/V/VI and VIII) and the cognitive module (posterior part of Crus I and Crus II), as well as the medial region of lobule IX. In addition, cognitive module showed higher value (red in Figures 4a,b) than motor module (blue in Figures 4a,b). In other words, according to Figure 4a, the values larger than zeros were mainly located in the cognitive module (posterior part of Crus I and Crus II, which corresponds to the default mode network, namely DMN), and the values less than zeros were mainly located in the motor module.

Compared with the controls, decreased gradient values in IGE were found in cerebellar lobules I–IV/V/VI and right CrusII/VIIb/IX in IGE (two-tailed t-test; FDR, $p < .05$). Moreover, increased gradient value was in left Crus I/VIIa and bilateral VIIb in patients with IGE (two-tailed *t*-test; FDR, $p < .05$). There was extensive functional compression in cerebellar SMN and DMN regions (Table S3 for details).

Furthermore, as shown in the scatter plot, the increased gradient value in the IGE was located at the lowest pole of the principal gradient (corresponding to the sensory-motor network), and the decreased value was located at the middle and the highest pole of the principal gradient (corresponding to DMN).

To better characterize the altered spatial pattern of sensorimotor-supramodal hierarchical gradient changed by IGE, a global histogram analysis was carried out, and was shown in Figure 4c. Through the nonparametric permutation test, it was found that the distance between the two peaks of IGE was significantly compressed, that is, the distance between SMN and DMN was significantly shortened (permutation 5000 times, $p = .03$).

3.3 | Fusion between functional gradient and motor components

The four cerebellar motor components had different contributions to the cerebello–cerebral gradient in both groups (Figure 5a,b). In short, the contribution of left primary motor and SMA components to gradient was mainly found in the cerebellar motor module; however, cognitive module (local region in Crus I/II) showed significant contribution to the gradients. Compared with the controls, IGE showed the increased contribution of left sensorimotor component to gradient in the right cerebellum Crus I (Figure 5c). On the contrary, the decreased contribution of right sensorimotor components was observed in bilateral medial cerebellum VI and cerebellar Crus I/II. Interestingly, only the enhanced contribution of SMA to the cerebello–cerebral gradient was in cerebellar motor region (cerebellar lobule VI). There was no

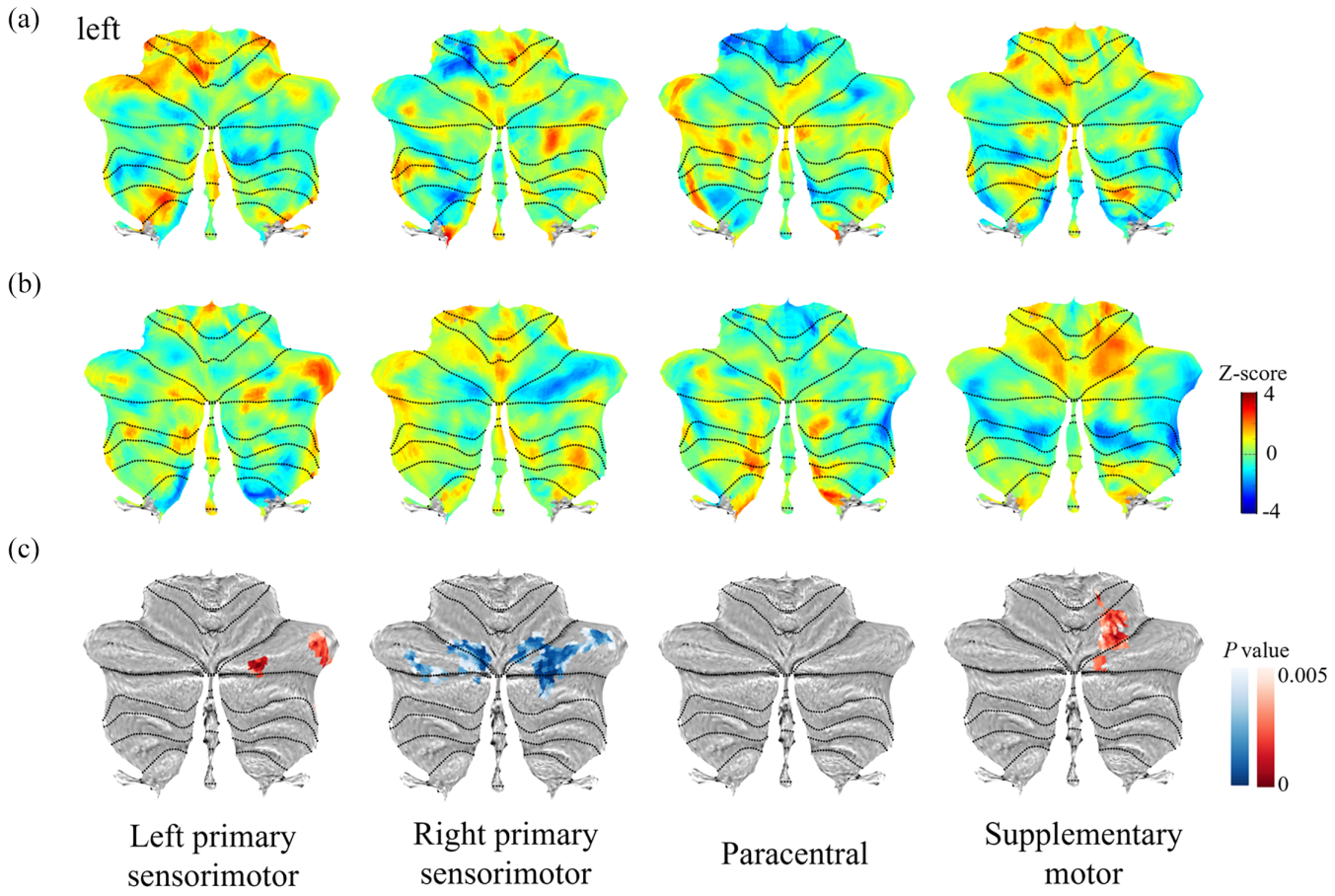

FIGURE 5 Fusion between cerebellar motor components and functional gradient (population covariance). (a) β maps of the normal control group. (b) β maps of the IGE group. (c) The difference in contribution between the control and IGE group (permutation test, $p < .005$). The red represents the increased β, while blue represents a decrease in contribution in patients. In (a,b), the β maps were standardized by Z-score.

significant difference between the two groups in the contribution of the paracentral component to the gradient (Table S4 for details).

In addition, using the voxel-based covariance, four motor components illustrated significant contributions to the gradient in both groups. However, there was only a significantly decreased contribution of the right primary sensorimotor region to the gradient in patients ($t = -2.06$; $p = .04$) (Figure S3).

3.4 | Correlation with clinical variables

When analyzing the correlation between abnormal cerebellar motor components and clinical variables, considering the confounding effect of gender, age of the onset, and drugs on the results, this study took gender, age of the onset, and whether to take drugs as covariates, and only observed that the mapping value of VIIb in the left cerebellar lobule of cerebellar motor component SMA was positively correlated with disease duration ($p < .05$) (Figure 6a). Similar to the former, the altered gradient score of left cerebellar lobule V was also positively correlated with the course of the disease (Figure 6b). The verification results were similar to the above results. See Figures S4–S6 for details.

4 | DISCUSSION

This study combined the functional gradient and ICA for cerebello–cerebral FC to investigate functional integration in motor system. Consistent with previous studies (Buckner, 2013; King et al., 2019; Middleton & Strick, 2001), the current study revealed motor functional modules were closely related with cerebral motor components. The altered mapping of cerebral motor components to cerebellum was observed in motor module in patients with IGE. In addition, the contribution of primary motor in dominant hemisphere (left dominant hemisphere for right-handedness) to gradient was mainly located in the cerebellar motor module rather than the nondominant hemisphere in healthy subjects, suggesting the lateralization for functional segregation of the unimodal network in cerebellum. In IGE, the gradient analysis exhibited functional compression in cerebello–cerebral FC. Interestingly, the contribution of the motor components to the gradient was unbalanced between bilateral primary sensorimotor components in patients: the increase was observed in cerebellar cognitive module for the dominant hemisphere (left) cerebral primary sensorimotor), but the decrease was found in the cerebellar cognitive module for the undominant hemisphere (right) primary sensorimotor.

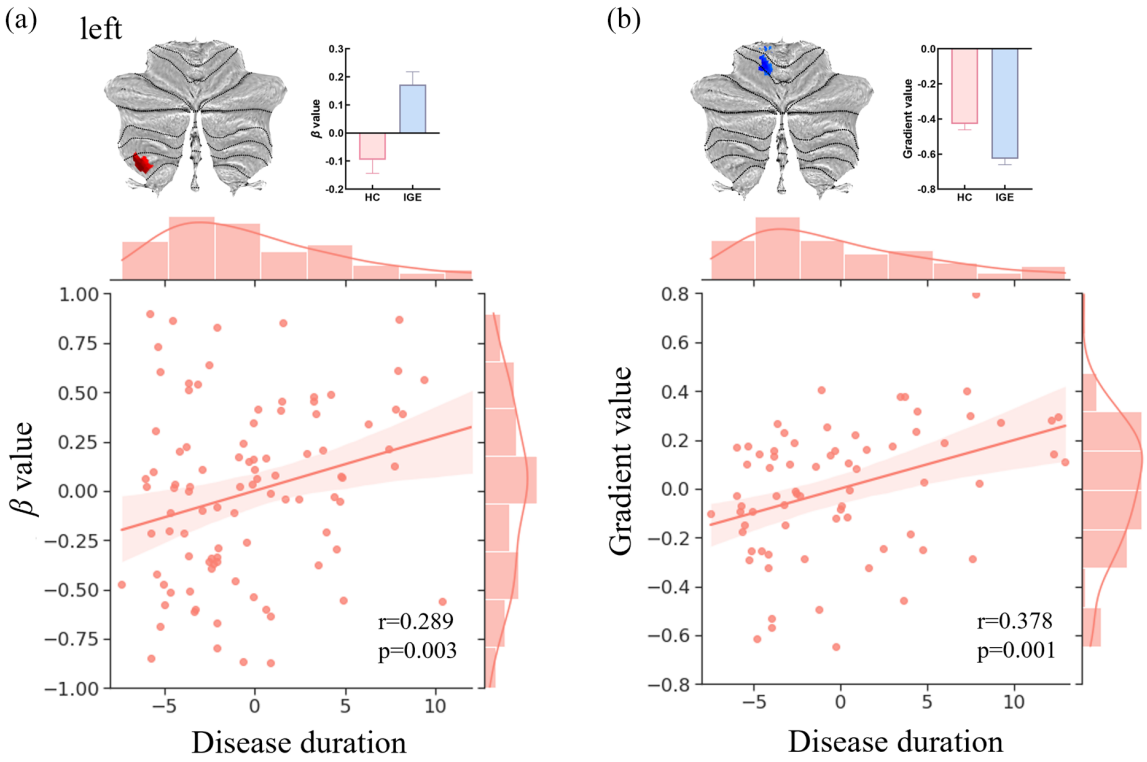

FIGURE 6 Correlation analysis between the altered value and disease duration. (a) Correlation between the abnormal cerebellar motor component (SMA) and disease duration. Significant positive correlations between disease duration and mapping values (β) of left cerebellar lobule VIIb. (b) Correlation between the altered gradient scores and disease duration. Significant positive correlations between disease duration and gradient value of left cerebellar lobule V. The bar chart in the figure was the mean of β and the gradient value in the areas significantly related to the course of the disease.

These findings substantially contributed to the functional integration evidence to understand the motor functional abnormality in patients with IGE.

4.1 | Cerebello–cerebral cortex integration

Anatomical and functional neuroimaging studies have confirmed that the cerebellum included motor and cognitive functional modules, and was connected to the cerebral cortex through the superior cerebellar peduncle (Duan et al., 2015; He et al., 2019; Middleton & Strick, 1994; Middleton & Strick, 2001). Using two different functional analysis strategies based on resting-state fMRI, this study identified two functional integration models between cerebrum and cerebellum for motor and cognitive modules, respectively. The finding would provide comprehensive evidence for revealing the characteristics of cerebellar function.

The motor module of the cerebellum mainly involves the cerebellar lobule, directly involved in motor coordination and related motor learning (Fine et al., 2002). Previous fMRI studies based on task states have shown that the cerebellum anterior lobules (I–IV/V) could be activated through motor task paradigm (Stoodley et al., 2012; Stoodley & Schmahmann, 2009, 2010; Zhang et al., 2023). Cerebellar lobule VII is also considered as an important motor region (Buckner et al., 2011; Guell, Gabrieli, & Schmahmann, 2018). Consistent with these findings, by ICA exploring the integration of cerebello–cerebrum FC, the mapping of the four cerebral motor components to the cerebellum involved cerebellar motor module with positive connectivity and cognitive module with negative connectivity. This finding suggests that cerebellar motor clusters were the main region involved in the integration of cerebello–cerebrum motor functions. In addition, more and more evidence also illustrated the hemispheric differences in sensory-motor networks of the healthy population at the structural and functional level (Barber et al., 2012; Mattay et al., 1998; Mutha et al., 2013). Our findings implicate the contralateral mapping of primary sensorimotor in the cerebellum, especially in the major motor areas (VI and VIII lobules). Thus, the additional analysis of the cerebro–cerebellum FC would provide an efficient approach to evaluate motor functional integration.

In addition, through the gradient analysis, the motor and cognitive modules were also divided into two ends: motor on negative end and cognition on positive end. According to the cerebellar activation induced by cognitive tasks, it was found that the cerebellar cognitive modules were mainly located at the junction of Crus I, Crus II, and cerebellar lobules IX/X (Diedrichsen & Zotow, 2015). Moreover, the mapping of the three brain motor components to the cerebellum included the lateral Crus I through the integration of cerebello–cerebrum motor function, suggesting that Crus I may have a hand in the regulation of

motor and cognitive function. By studying the role of motor system in working memory, Marvel and his colleagues stated that Crus I may be used as a "secondary motor" region to represent the intersection of cerebellar motor and cognitive function (Marvel et al., 2019). The findings probably reflected a convergence nature of cerebellar Crus I in the dimension of motor to nonmotor processing in cerebello–cerebral functional integration.

Actually, the gradient analysis for cerebro–cerebellar FC matrixes would reflect that the cerebellum and cerebral cortex share a similar macroscale principle of organization (Dong et al., 2020; Guell, Schmahmann, et al., 2018). The proposed linear fusion for gradient analysis with motor components could evaluate the contribution of motor function to the hierarchical organization, which was considered as an intrinsic feature of cerebellum and cerebral cortex. Interestingly, the primary motor in dominant hemisphere (left for right-handed) to gradient was mainly located in the cerebellar motor module rather than the nondominant hemisphere, suggesting the lateralization for functional segregation of the unimodal network in cerebellum.

4.2 | Disturbance of modules from motor to non-motor in IGE

Patients with IGE showed reduced mapping of SMA to cerebellar lobule VI. The finding might reflect the weakened interaction of cerebellar higher-cerebral primary functions in patients. Besides, the decreased mapping of SMA in lobule VI might also lead to fine motor and balance disorders in patients (Fine et al., 2002; Shima & Tanji, 1998). It might implicate that the inhibitory output of cerebellum to SMA is weakened, which may contribute to the high excitability of the epileptic motor cortex. A previous study has shown that the functional and structural connection between cerebellum and SMA was decreased in patients with IGE (Zhang, Huang, Liu, et al., 2021), which is speculated to be related to motor dysfunction symptoms during seizures (Stoodley & Schmahmann, 2010; Zhang, Huang, Liu, et al., 2021). Controlling the output of cerebellar cortex can effectively inhibit abnormal epileptic discharges. Interestingly, the contribution of SMA to the gradient value of right cerebellar lobule VI increased, indicating that the mapping of SMA in the cerebellum over involved the overall cerebello–cerebrum functional gradient. Similarly, the abnormal contribution of other cerebellar motor components to the functional gradient may be the excessive involvement of cerebellar motor components in the overall functional gradient. Therefore, the results related the SMA components further shed light on that the cerebello–cerebral integration might be insufficient in the collaborative processing of sensory-motor information, which may be related to the dysfunction of motor system caused by long-term seizures.

The mapping of SMA to lobule VIIIb in cerebellum increased in this study. This difference may represent pathological abnormalities or compensatory reorganization changes in IGE patients compared with controls. The correlation between β value of VIIIb and the course of the disease supports the former possibility (pathological changes rather than compensatory reorganization changes), because the longer disease duration will be accompanied by more obvious changes compared with the early stage of the disease, which may be a cumulative injury. However, the compensatory recombination changes may occur in those subjects with the most severe clinical injury or the longest disease progression. Significantly, the increased mapping of left primary sensorimotor with the left cerebellar lobule was not related to clinical variables. This research speculates that this increased mapping may be a compensatory recombination change. The gradient value of left cerebellar lobule V was significantly positively correlated with the disease duration. However, this explanation needs to be further confirmed, as the study did not conduct longitudinal research and there are large inter-individual differences.

4.3 | Altered mapping of convergence in IGE

The first convergence finding was a decrease in both left primary sensorimotor and paracentral components mapping cerebellar lobular area VIIIa in patients with IGE. As convergence findings, the decreased mapping of cerebellar lobule VIIa may reveal that the decline of cognitive function, especially memory ability, in patients with IGE may be related to the impairment of lobule VIIIa. It also indicates that cerebellar damage in patients may lead to motor and cognitive dysfunction. In addition, the analysis based on gradient density histogram in this study found gradient functional compression in patients, mainly due to the reduction of gradient sensorimotor and cognitive functional separation. The compression of motor function was mainly manifested in the increase of gradient values of bilateral cerebellar lobules VIIa and the lateral side of left Crus I in the convergence. This further suggests that the functional hierarchy of cerebellum in patients with IGE is destroyed.

The contribution of the motor components to the gradient was unbalanced between bilateral primary sensorimotor components in patients. The increase was observed in cerebellar cognitive module (cerebellar lobules VIIb/VIII) for the left cerebral primary sensorimotor, but the decrease was found in the cerebellar cognitive module for the right primary sensorimotor. The unbalance may be related to the feature of motor dominant hemisphere. In this study, all subjects were right-handed. Studies have shown that non-dominant hand movements, perhaps because they are less "automatic", appear to require more cortical activity, resulting in more recruitment of the ipsilateral cerebellum (Mattay et al., 1998). Moreover, seizures may allow the propagation of abnormal neuronal activity to adversely affect the epileptic hemisphere, leading patients to rely more on the sensorimotor cortex of the contralateral hemisphere (Woodward et al., 2014). This also explains that the increased mapping of the right primary sensorimotor area in the left cerebellar motor area may be a compensatory mechanism for the non-dominant hemisphere of the cerebellum. Patients with IGE need this non-dominant hemisphere compensation to maintain their motor function. This suggests that BOLD activity in the right sensorimotor area was increased in patients compared with normal subjects. Danguecan et al. pointed out that in the setting of early-onset epilepsy, the disruption of specialization in canonical

language regions can compensate for the impaired regions in the dominant hemisphere by recruiting undamaged regions in the contralateral hemisphere (Danguecan & Smith, 2019). Likewise, ictal or interictal dyskinesias in patients can compensate for impaired motor-related areas in the dominant hemisphere by recruiting more undamaged areas in the contralateral hemisphere. Taken together, this provides evidence for understanding the physiological and pathological mechanism of general tonic–clonic seizures from a new perspective.

There are several limitations to this study. First, although age and gender were regressed as uninteresting covariates in the statistical process, we still cannot completely exclude the potential impact. Second, our study did not rule out the confounding effects of AED treatment. Although all patients were asked not to take their medicine on the day of scanning, the possible contributions of AED medications to the motor cortex might be included. The duration and dose of taking medicine were not equal, thus the effects of AED differed across patients, which might confuse the FC findings. In the future study, drug-naive epilepsy patients would be collected to avoid interference with AED. Finally, we collected resting-state fMRI data rather than task-induced fMRI for patients. Designing the task during fMRI would be considered to further explore the motor-damaged brain regions in patients with IGE.

5 | CONCLUSION

This study reveals the interrupted integration between cerebellum and cerebral motor network in patients with IGE, implicating that cerebello–cerebral integration might be insufficient in the collaborative processing of sensorimotor information in patients. This finding provides preliminary insights into the underlying pathophysiological mechanism of IGE. The proposed fusion framework encourages more research to pay attention to IGE motor abnormality and their abnormal interaction with cognition, to deepen our understanding of this disease.

ACKNOWLEDGEMENT

We thankfully acknowledge participaton of subjests.

FUNDING INFORMATION

This work was supported by a grant from the National Nature Science Foundation of China (61933003, U2033217, 62201133, and 81960249), China Postdoctoral Science Foundation (2021TQ0061), Chengdu Science and Technology Bureau (2021-YF09-00107-SN), and the CAMS Innovation Fund for Medical Sciences (CIFMS) (No. 2019-I2M-5-039).

CONFLICT OF INTEREST STATEMENT

The authors declare no conflicts of interest.

DATA AVAILABILITY STATEMENT

The data that support the findings of this study are available on request from the corresponding author. The data are not publicly available due to privacy or ethical restrictions.

ORCID

Sisi Jiang https://orcid.org/0000-0002-7430-9639
Cheng Luo https://orcid.org/0000-0003-0524-5886

REFERENCES

Barber, A. D., Srinivasan, P., Joel, S. E., Caffo, B. S., Pekar, J. J., & Mostofsky, S. H. (2012). Motor "dexterity"?: Evidence that left hemisphere lateralization of motor circuit connectivity is associated with better motor performance in children. *Cerebral Cortex*, *22*(1), 51–59.

Buckner, R. L. (2013). The cerebellum and cognitive function: 25 years of insight from anatomy and neuroimaging. *Neuron*, *80*(3), 807–815.

Buckner, R. L., Krienen, F. M., Castellanos, A., Diaz, J. C., & Yeo, B. T. T. (2011). The organization of the human cerebellum estimated by intrinsic functional connectivity. *Journal of Neurophysiology*, *106*(5), 2322–2345.

Coifman, R. R., Lafon, S., Lee, A. B., Maggioni, M., Nadler, B., Warner, F., & Zucker, S. W. (2005). Geometric diffusions as a tool for harmonic analysis and structure definition of data: Diffusion maps. *Proceedings of the National Academy of Sciences of the United States of America*, *102*(21), 7426–7431.

Danguecan, A. N., & Smith, M. L. (2019). Re-examining the crowding hypothesis in pediatric epilepsy. *Epilepsy & Behavior*, *94*, 281–287.

Diedrichsen, J. (2006). A spatially unbiased atlas template of the human cerebellum. *NeuroImage*, *33*(1), 127–138.

Diedrichsen, J., & Zotow, E. (2015). Surface-based display of volume-averaged cerebellar imaging data. *PLoS One*, *10*(7), e0133402.

Dong, D., Luo, C., Guell, X., Wang, Y., He, H., Duan, M., Eickhoff, S. B., & Yao, D. (2020). Compression of cerebellar functional gradients in schizophrenia. *Schizophrenia Bulletin*, *46*(5), 1282–1295.

Dong, L., Luo, C., Liu, X., Jiang, S., Li, F., Feng, H., Li, J., Gong, D., & Yao, D. (2018). Neuroscience information toolbox: An open source toolbox for EEG-fMRI multimodal fusion analysis. *Frontiers in Neuroinformatics*, *12*, 56.

Duan, M. J., Chen, X., He, H., Jiang, Y., Jiang, S., Xie, Q., Lai, Y., Luo, C., & Yao, D. (2015). Altered basal ganglia network integration in schizophrenia. *Frontiers in Human Neuroscience*, *9*, 561.

Fine, E. J., Ionita, C. C., & Lohr, L. (2002). The history of the development of the cerebellar examination. *Seminars in Neurology*, *22*(4), 375–384.

Fisher, R. S., Cross, J. H., French, J. A., Higurashi, N., Hirsch, E., Jansen, F. E., Lagae, L., Moshé, S. L., Peltola, J., Roulet Perez, E., Scheffer, I. E., & Zuberi, S. M. (2017). Operational classification of seizure types by the international league against epilepsy: Position paper of the ILAE Commission for Classification and Terminology. *Epilepsia*, *58*(4), 522–530.

Guell, X., Gabrieli, J. D. E., & Schmahmann, J. D. (2018). Triple representation of language, working memory, social and emotion processing in the cerebellum: Convergent evidence from task and seed-based resting-state fMRI analyses in a single large cohort. *NeuroImage*, *172*, 437–449.

Guell, X., Schmahmann, J. D., Gabrieli, J. D., & Ghosh, S. S. (2018). Functional gradients of the cerebellum. *eLife*, *7*, e36652.

Guo, S., Lin, Y., Zhao, S., Cui, Y., Xia, Y., Chen, K., Yao, D., & Guo, D. (2023). Pattern recognition of schizophrenia based on multidimensional spatial feature fusion. *Brain-Apparatus Communication: A Journal of Bacomics*, *2*(1), 2249036.

He, H., Luo, C., Luo, Y., Duan, M., Yi, Q., Biswal, B. B., & Yao, D. (2019). Reduction in gray matter of cerebellum in schizophrenia and its influence on static and dynamic connectivity. *Human Brain Mapping*, *40*(2), 517–528.

Huntenburg, J. M., Bazin, P. L., & Margulies, D. S. (2018). Large-scale gradients in human cortical organization. *Trends in Cognitive Sciences*, *22*(1), 21–31.

Kelly, R. M., & Strick, P. L. (2003). Cerebellar loops with motor cortex and prefrontal cortex of a nonhuman primate. *Journal of Neuroscience*, *23*(23), 8432–8444.

King, M., Hernandez-Castillo, C. R., Poldrack, R. A., Ivry, R. B., & Diedrichsen, J. (2019). Functional boundaries in the human cerebellum

revealed by a multi-domain task battery. *Nature Neuroscience*, *22*(8), 1371–1378.

Knosche, T. R., & Tittgemeyer, M. (2011). The role of long-range connectivity for the characterization of the functional-anatomical organization of the cortex. *Frontiers in Systems Neuroscience*, *5*, 58.

Krauss, G. L., & Koubeissi, M. Z. (2007). Cerebellar and thalamic stimulation treatment for epilepsy. *Acta Neurochirurgica. Supplement*, *97*(Pt 2), 347–356.

Liu, G. H., Lyu, G. W., Yang, N., Chen, B., Yang, J., Hu, Y., Lei, Y., Xia, J., Lin, F., & Fan, G. (2019). Abnormalities of diffusional kurtosis imaging and regional homogeneity in idiopathic generalized epilepsy with generalized tonic-clonic seizures. *Experimental and Therapeutic Medicine*, *17*(1), 603–612.

Luo, C., Li, Q., Xia, Y., Lei, X., Xue, K., Yao, Z., Lai, Y., Martı´nez-Montes, E., Liao, W., Zhou, D., Valdes-Sosa, P. A., Gong, Q., & Yao, D. (2012). Resting state basal ganglia network in idiopathic generalized epilepsy. *Human Brain Mapping*, *33*(6), 1279–1294.

Luo, C., Zhang, X. X., Cao, X., Gan, Y., Li, T., Cheng, Y., Cao, W., Jiang, L., Yao, D., & Li, C. (2016). The lateralization of intrinsic networks in the aging brain implicates the effects of cognitive training. *Front Aging Neurosci*, *8*, 32.

Margulies, D. S., Ghosh, S. S., Goulas, A., Falkiewicz, M., Huntenburg, J. M., Langs, G., Bezgin, G., Eickhoff, S. B., Castellanos, F. X., Petrides, M., Jefferies, E., & Smallwood, J. (2016). Situating the default-mode network along a principal gradient of macroscale cortical organization. *Proceedings of the National Academy of Sciences of the United States of America*, *113*(44), 12574–12579.

Marvel, C. L., Morgan, O. P., & Kronemer, S. I. (2019). How the motor system integrates with working memory. *Neuroscience and Biobehavioral Reviews*, *102*, 184–194.

Mattay, V. S., Callicott, J. H., Bertolino, A., Santha, A. K. S., van Horn, J. D., Tallent, K. A., Frank, J. A., & Weinberger, D. R. (1998). Hemispheric control of motor function: A whole brain echo planar fMRI study. *Psychiatry Research-Neuroimaging*, *83*(1), 7–22.

Middleton, F. A., & Strick, P. L. (1994). Anatomical evidence for cerebellar and basal ganglia involvement in higher cognitive function. *Science*, *266*(5184), 458–461.

Middleton, F. A., & Strick, P. L. (2001). Cerebellar projections to the prefrontal cortex of the primate. *Journal of Neuroscience*, *21*(2), 700–712.

Mutha, P. K., Haaland, K. Y., & Sainburg, R. L. (2013). Rethinking motor lateralization: Specialized but complementary mechanisms for motor control of each arm. *PLoS One*, *8*(3), e58582.

Scheffer, I. E., Berkovic, S., Capovilla, G., Connolly, M. B., French, J., Guilhoto, L., Hirsch, E., Jain, S., Mathern, G. W., Moshé, S. L., Nordli, D. R., Perucca, E., Tomson, T., Wiebe, S., Zhang, Y. H., & Zuberi, S. M. (2017). ILAE classification of the epilepsies: Position paper of the ILAE Commission for Classification and Terminology. *Epilepsia*, *58*(4), 512–521.

Shima, K., & Tanji, J. (1998). Both supplementary and presupplementary motor areas are crucial for the temporal organization of multiple movements. *Journal of Neurophysiology*, *80*(6), 3247–3260.

Stoodley, C. J., & Schmahmann, J. D. (2009). Functional topography in the human cerebellum: A meta-analysis of neuroimaging studies. *NeuroImage*, *44*(2), 489–501.

Stoodley, C. J., & Schmahmann, J. D. (2010). Evidence for topographic organization in the cerebellum of motor control versus cognitive and affective processing. *Cortex*, *46*(7), 831–844.

Stoodley, C. J., Valera, E. M., & Schmahmann, J. D. (2012). Functional topography of the cerebellum for motor and cognitive tasks: An fMRI study. *NeuroImage*, *59*(2), 1560–1570.

Tangwiriyasakul, C., Perani, S., Centeno, M., Yaakub, S. N., Abela, E., Carmichael, D. W., & Richardson, M. P. (2018). Dynamic brain network states in human generalized spike-wave discharges. *Brain*, *141*(10), 2981–2994.

Vollmar, C., O'Muircheartaigh, J., Barker, G. J., Symms, M. R., Thompson, P., Kumari, V., Duncan, J. S., Janz, D., Richardson, M. P., & Koepp, M. J. (2011). Motor system hyperconnectivity in juvenile myoclonic epilepsy: A cognitive functional magnetic resonance imaging study. *Brain*, *134*(Pt 6), 1710–1719.

Woodward, K. E., Gaxiola-Valdez, I., Mainprize, D., Grossi, M., Goodyear, B. G., & Federico, P. (2014). Recent seizure activity alters motor organization in frontal lobe epilepsy as revealed by task-based fMRI. *Epilepsy Research*, *108*(8), 1286–1298.

Yuan, R., Di, X., Taylor, P. A., Gohel, S., Tsai, Y.-H., & Biswal, B. B. (2016). Functional topography of the thalamocortical system in human. *Brain Structure and Function*, *221*, 1971–1984.

Zhang, X., Liu, C., Weng, Z., & Lu, B. (2023). The corticomuscular coupling underlying movement and its application for rehabilitation: A review. *Brain-Apparatus Communication: A Journal of Bacomics*, *2*(1), 1–16.

Zhang, Y., Huang, G., Liu, M., Li, M., Wang, Z., Wang, R., & Yang, D. (2021). Functional and structural connective disturbance of the primary and default network in patients with generalized tonic-clonic seizures. *Epilepsy Research*, *174*, 106595.

Zhu, L., Li, Y. B., Wang, Y. F., Li, R., Zhang, Z., Lu, G., & Chen, H. (2016). Aberrant long-range functional connectivity density in generalized tonic-clonic seizures. *Medicine*, *95*(24), e3893.

SUPPORTING INFORMATION

Additional supporting information can be found online in the Supporting Information section at the end of this article.

How to cite this article: Chen, J., Jiang, S., Lu, B., Liao, J., Yang, Z., Li, H., Pei, H., Li, J., Iturria-Medina, Y., Yao, D., & Luo, C. (2024). The role of the primary sensorimotor system in generalized epilepsy: Evidence from the cerebello–cerebral functional integration. *Human Brain Mapping*, *45*(1), e26551. https://doi.org/10.1002/hbm.26551